

**DEVELOPMENT OF POLYANILINE/POLYIMIDE COMPOSITE AS A  
HEAT RESISTANT GAS SENSOR**



Ms. Sutthida Watcharaphalakorn

A Thesis Submitted in Partial Fulfilment of the Requirements  
for the Degree of Master of Science  
The Petroleum and Petrochemical College, Chulalongkorn University  
in Academic Partnership with  
The University of Michigan, The University of Oklahoma,  
and Case Western Reserve University


2002

ISBN 974-03-1611-5


**Thesis Title** : Development of Polyaniline/Polyimide Composite as a Heat Resistant Gas Sensor  
**By** : Ms. Sutthida Watcharaphalakorn  
**Program** : Polymer Science  
**Thesis Advisors** : Assoc. Prof. Anuvat Sirivat  
Prof. Johannes Schwank

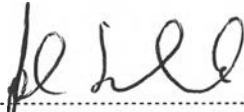
---

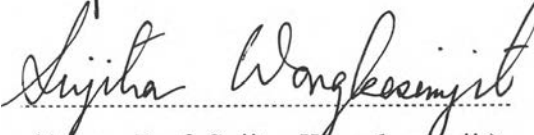
Accepted by the Petroleum and Petrochemical College, Chulalongkorn University, in partial fulfilment of the requirements for the Degree of Master of Science.

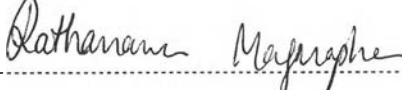
  
..... College Director  
(Assoc. Prof. Kunchana Boonyakiat)

**Thesis Committee:**

  
.....  
(Assoc. Prof. Anuvat Sirivat)

  
.....  
(Prof. Johannes Schwank)

  
.....  
(Assoc. Prof. Sujitra Wongkasemjit)

  
.....  
(Asst. Prof. Rathanawan Magaraphan)

**ABSTRACT**

4372021063 : POLYMER SCIENCE PROGRAM

Sutthida Watcharaphalakorn: Development of Polyaniline/  
Polyimide Composite as a Heat Resistant Gas Sensor

Thesis Advisors: Assoc. Prof. Anuvat Sirivat and Prof. Johannes  
Schwank, 116 pp. ISBN 974-03-1611-5

Keywords : Conducting polymer/Polyaniline and derivatives/Polyimide/Sensor/  
Composite/Thermal stability.

Polyaniline (PANI)-based gas sensor was modified to be used at high temperature by dispersing PANI in an insulating polyimide (PI) matrix using a dry mixing method. The effect of acid dopant type, acid concentration and thermal stability on exposure of the modified sensor to CO gas was studied. At the fully doping level, the camphorsulfonic acid-doped PANI had higher specific conductivity than the nitric acid-doped PANI. The conductivity response to CO,  $\Delta\sigma$ , followed the power law  $\Delta\sigma = a[\text{CO}]^b$  where the scaling exponent  $b$  characterizes the concentration dependence ( $d\Delta\sigma/dc$ ). At increasing doping levels, the concentration dependence increased and the temporal response time became shorter. At high temperatures, the PANI/PI composite had greater concentration dependence than the doped PANI. The conductivity response correlated well with the morphology and thermal stability as determined by EA, FT-IR, EDX, UV-Vis., XRD, SEM and TGA.

## บทคัดย่อ

นางสาวสุทธิดา วัชรพลากร : การพัฒนาพอลิเมอร์ผสมระหว่างพอลิอนิลีนและพอลิอิมิดสำหรับตรวจวัดก๊าซคาร์บอนมอนอกไซด์ที่เสถียรที่อุณหภูมิสูง (Development of Polyaniline/polyimide Composite as a Heat Resistant Gas Sensor) อ.ที่ปรึกษา : ศ. ดร. โจฮานเนสชแวงค์ และ รศ.ดร. อนุวัฒน์ สิริวัฒน์ 116 หน้า ISBN 974-03-1611-5

อุปกรณ์ตรวจวัดก๊าซที่ประกอบด้วยพอลิอนิลีนสามารถปรับปรุงให้มีความเสถียรต่อความร้อนได้โดยนำมาผสมโดยการบดกับสารที่ทำหน้าที่เป็นฉนวนคือพอลิอิมิด โดยทำการศึกษาผลของชนิดของกรดตัวโต๊ปและความเข้มข้นของกรดตัวโต๊ปต่อสมบัติการนำไฟฟ้าเมื่อทำการตรวจวัดก๊าซคาร์บอนมอนอกไซด์ จากการศึกษาพบว่า เมื่อโต๊ปพอลิอนิลีนให้ถึงระดับสูงสุดกรด แคมปอร์ซัลฟอริกให้ค่าการนำไฟฟ้าที่สูงกว่ากรดไนตริก, การตอบสนองต่อไฟฟ้าเมื่อทำการตรวจวัดก๊าซคาร์บอนมอนอกไซด์ ได้สมการความสัมพันธ์  $\Delta\sigma = a[\text{CO}]^b$  เมื่อ a คือจุดตัดแกน และ b คือความชันของกราฟและสัมพันธ์กับค่าความแปรผันต่อความเข้มข้น ค่าความแปรผัน ต่อความเข้มข้นเพิ่มขึ้นเมื่อระดับของการโต๊ปเพิ่มขึ้นและเวลาที่ใช้ในการตอบสนองเร็วขึ้นวัสดุ ลูกผสมระหว่างพอลิอนิลีนและพอลิอิมิดมีค่าความแปรผันต่อความเข้มข้นที่ดีขึ้นเมื่อเทียบกับพอลิอนิลีน นอกจากนี้ยังพบอีกว่าค่าการนำไฟฟ้ามีความสัมพันธ์กับลักษณะโครงสร้างและความ เสถียรทางไฟฟ้าซึ่งสามารถอธิบายได้โดยการจำแนกโดยวิธี EA, FT-IR, EDX, UV-Vis., XRD, SEM และ TGA.

## ACKNOWLEDGEMENTS

The author would like to express her sincere thank to all instructors who have taught the invaluable knowledge to her especially Assoc. Prof. Anuvat Sirivat and Prof. Johannes Schwank, her advisors, who always advise and suggest throughout this thesis work.

Also, she would like to express her respectful thank to C.P.O. Poon Arjpru for all his works and suggestion on all technical problems. Special thank is extended to her entire friends at the Petroleum and Petrochemical College, Chulalongkorn University for their help, suggestions and encouragements, especially, Ms. Chintana Chuapradit for her good role as a colleague. In addition, she would like to acknowledge Ms. Ladawan Ruangchuay, Mr. Wanchai Lerdwijitjarud, Ms. Datchanee Chotpattananont and all Ph.D. students for their help, suggestion, interesting ideas and discussion on both technical and paper works on this thesis. Moreover, sincere thank is also extended to all members and staffs at the Petroleum and Petrochemical College, Chulalongkorn University for providing the valuable equipment, instrument training and utilization.

Finally, the sincerest appreciation is expressed to her family for the love, care, understanding and encouragement throughout her life.

## TABLE OF CONTENTS

	<b>PAGE</b>
Title Page	i
Abstract (in English)	iii
Abstract (in Thai)	iv
Acknowledgements	v
Table of Contents	vi
List of Tables	ix
List of Figures	xii
List of Schemes	xv
 <b>CHAPTER</b>	
<b>I INTRODUCTION</b>	<b>1</b>
1.1 Introduction	1
1.2 Background	2
 <b>II LITERATURE SURVEY</b>	 <b>7</b>
2.1 Polyaniline	7
2.2 Polymer Blend as Conductive Polymer	9
2.3 Polyimide as Conductive Blend	11
 <b>III EXPERIMENTAL</b>	 <b>13</b>
3.1 Materials	13
3.2 Methodology	13
3.2.1 Polyaniline Synthesis and Doping Process	13
3.2.2 Polyimide Synthesis	15
3.2.3 Blend Preparation	16
3.2.4 Characterization	16
3.2.5 Conductivity Measurement	19

<b>CHAPTER</b>	<b>PAGE</b>
<b>IV RESULTS AND DISCUSSION</b>	23
4.1 Characterization	23
4.1.1 Polyaniline	23
4.1.2 Polyimide	32
4.1.3 Polyaniline/Polyimide Composites	35
4.2 Electrical Conductivity Property	37
4.2.1 Effect of Acid Dopant Type and Concentration	37
4.2.2 Effect of the Crystallinity	39
4.2.3 Effect of Amount of Polyimide in the Blend	41
4.3 Conductivity Response and Interaction to CO	43
4.3.1 Doped Polyaniline	45
4.3.2 Doped Polyaniline Composite with Polyimide	52
<b>V CONCLUSIONS</b>	62
<b>REFERENCES</b>	63
<b>APPENDICES</b>	
<b>Appendix A</b> Determination of PANI and PI molecular structure from elemental analysis	66
<b>Appendix B</b> Calculation of doping level from elemental analysis of the doped polyaniline	68
<b>Appendix C</b> Identification of characteristic FT-IR peaks of synthesized polyaniline and polyimide	71
<b>Appendix D</b> Calculation of doping level from FT-IR	74
<b>Appendix E</b> Calculation of doping level from EDX	77
<b>Appendix F</b> Identification of characteristic peaks of polyaniline from UV-Visible spectroscopy	79
<b>Appendix G</b> Raw data of percentage weight loss of PANI and PI and the composites by TGA	81

<b>CHAPTER</b>	<b>PAGE</b>
<b>Appendix H</b> Scanning electron micrograph of PANI and PI and composites	84
<b>Appendix I</b> Determination of crystallinity percentage from XRD	88
<b>Appendix J</b> Determination of Ohm's law regime	91
<b>Appendix K</b> Determination of the geometric correction factor	94
<b>Appendix L</b> Conductivity measurement	98
<b>Appendix M</b> Conductivity measurement upon expose to CO	101
<b>CURRICULUM VITAE</b>	116



## LIST OF TABLES

TABLE	PAGE
4.1 Concentration dependence value (b) and the intercept (a) from the plot between $\Delta\sigma$ and [CO] (ppm) for CSA doped polyaniline ( $N_A/N_{EB} = 10$ ) at $25 \pm 2$ , $35 \pm 2$ , $45 \pm 2$ and $55 \pm 2$ °C	49
4.2 Concentration dependence value (b) and the intercept (a) from the plot between $\Delta\sigma$ and [CO] (ppm) for HNO <sub>3</sub> doped polyaniline ( $N_A/N_{EB} = 10$ ) at $25 \pm 2$ , $35 \pm 2$ , $45 \pm 2$ and $55 \pm 2$ °C	49
4.3 Temporal response time (minute) of CSA doped polyaniline ( $N_A/N_{EB} = 1$ and $10$ ) at $25 \pm 2$ , $35 \pm 2$ , $45 \pm 2$ and $55 \pm 2$ °C at [CO] = 1000 ppm	51
4.4 Temporal response time (minute) of HNO <sub>3</sub> doped polyaniline ( $N_A/N_{EB} = 1$ and $10$ ) at $25 \pm 2$ , $35 \pm 2$ , $45 \pm 2$ and $55 \pm 2$ °C at [CO] = 1000 ppm	51
4.5 Values of a-intercept of the curve $\Delta\sigma = a[\text{CO}]^b$ of pure and blend at various temperatures	57
4.6 Values of b-slope of the curve $\Delta\sigma = a[\text{CO}]^b$ of pure and blend at various temperatures	57
4.7 Temporal response time (minute) of CSA doped polyaniline ( $N_A/N_{EB} = 10$ ) pure and blend with 30 %wt polyimide at $25 \pm 2$ , $35 \pm 2$ , $45 \pm 2$ and $55 \pm 2$ °C at [CO] = 1000 ppm	60
4.8 Temporal response time (minute) of HNO <sub>3</sub> doped polyaniline ( $N_A/N_{EB} = 10$ ) pure and blend with 30 %wt polyimide at $25 \pm 2$ , $35 \pm 2$ , $45 \pm 2$ and $55 \pm 2$ °C at [CO] = 1000 ppm	60
A.1 Average numbers of mole in the molecular structures of PANI and PI from elemental analyses	67
B.1 Raw data from elemental analyses and the calculated % doping levels of HNO <sub>3</sub> doped polyaniline	69

<b>TABLE</b>	<b>PAGE</b>
B.2 Raw data from elemental analyses and the calculated % doping levels of CSA doped polyaniline	69
B.3 Calculated % doping level and the electrical conductivity of CSA and HNO <sub>3</sub> doped polyanilines	70
C.1 Assignment peaks for FT-IR absorption bands of undoped and doped polyanilines	71
C.2 Assignment of peaks for FT-IR absorption bands of synthesized polyimide	73
D.1 Doping level (%) of CSA doped polyaniline from FT-IR	75
D.2 Doping level (%) of HNO <sub>3</sub> doped polyaniline from FT-IR	76
E.1 Doping level (%) of CSA doped polyaniline from EDX	77
E.2 Doping level (%) of HNO <sub>3</sub> doped polyaniline from EDX	78
F.1 Assignment peaks of UV-Visible peaks of undoped and doped polyanilines	79
F.2 Summarized data from UV-Visible spectra of undoped and Doped polyanilines	80
G.1 Raw data of percentage weight loss of undoped and 10-CSA doped polyanilines	81
G.2 Raw data of percentage weight loss of undoped and 10-HNO <sub>3</sub> doped polyanilines	82
G.3 Raw data of percentage weight loss of poly(amic acid) and polyimide	82
G.4 Raw data of percentage weight loss of PANI-10CSA/PI composite	83
G.5 Raw data of percentage weight loss of PANI-10 HNO <sub>3</sub> /PI composite	83
H.1 Scanning electron micrograph of undoped, CSA and HNO <sub>3</sub> doped polyanilines (powder from; x 1500)	84

<b>TABLE</b>	<b>PAGE</b>
H.2 Scanning electron micrograph of polyimide, 10-CSA and 10-HNO <sub>3</sub> doped polyaniline/polyimide composite at various blend ratios (powder from; x 1500)	86
I.1 Values of 2θ, d-spacing (A) and Miller indices of emeraldine hydrochloride	88
I.2 Calculated crystallinity of CSA doped polyaniline	89
I.3 Calculated crystallinity of HNO <sub>3</sub> doped polyaniline	90
K.1 Sheet resistivity and thickness of standard sheet (SiO <sub>2</sub> )	95
K.2 Determination of K factor of the constructed four point probe meter (Probe CW1)	96
K.3 Determination of K factor of the constructed four point probe meter (Probe P_AO)	97
L.1 Raw data of conductivity measurement for CSA and HNO <sub>3</sub> doped polyanilines ( $N_A/N_{EB} = 10$ )	98
L.2 Raw data of conductivity measurement for CSA and HNO <sub>3</sub> doped polyanilines ( $N_A/N_{EB} = 10$ ) blend with PI at various blend ratios	100
M.1 Raw data of conductivity measurement upon exposure to CO for CSA and HNO <sub>3</sub> doped polyanilines at 25 °C	102
M.2 Raw data of conductivity measurement upon exposure to CO for CSA and HNO <sub>3</sub> doped polyanilines ( $N_A/N_{EB} = 10$ ) at 35, 45 and 55 °C	106
M.3 Raw data of conductivity measurement upon exposure to CO for CSA and HNO <sub>3</sub> doped polyanilines ( $N_A/N_{EB} = 10$ ) blend with 30 %wt polyimide at 25, 35, 45 and 55 °C	110

## LIST OF FIGURES

FIGURE	PAGE
1.1 Contribution of different sector of petrochemical industrial emission (Brett B.M., 1987)	1
1.2 Protonic acid doping and oxidative doping of polyaniline	4
1.3 Two-step synthesis of polyimide	5
4.1 Relationship between the % doping level and doping ratio of HNO <sub>3</sub> and CSA doped polyanilines	24
4.2 FT-IR spectra of undoped, HNO <sub>3</sub> and CSA doped polyanilines	25
4.3 Doping level (%) vs. doping ratio of CSA doped polyaniline	26
4.4 Doping level (%) vs. doping ratio of HNO <sub>3</sub> doped polyaniline	27
4.5 UV-visible spectra of undoped, HNO <sub>3</sub> and CSA doped polyanilines	29
4.6 TGA thermogram of undoped, HNO <sub>3</sub> and CSA doped polyanilines	30
4.7 XRD patterns of undoped, HNO <sub>3</sub> and CSA doped polyanilines	31
4.8 FT-IR spectra of PAA and PI	33
4.9 TGA thermogram of PAA and PI	34
4.10 TGA thermogram of CSA doped polyaniline blend with polyimide at various %wt of PI in the blend	35
4.11 TGA thermogram of HNO <sub>3</sub> doped polyaniline blend with polyimide at various %wt of PI in the blend	36
4.12 Conductivity vs. % doping level of CSA and HNO <sub>3</sub> doped polyaniline ( $N_A/N_{EB} = 0.2, 0.5, 1.0, 2.0, 5.0, 10.0$ and $20.0$ ).	37
4.13 $\sigma$ /% doping level vs. the crystallinity of CSA and HNO <sub>3</sub> doped polyanilines ( $N_A/N_{EB} = 0.2, 0.5, 1.0, 2.0, 5.0, 10.0$ and $20.0$ )	39

<b>FIGURE</b>	<b>PAGE</b>
4.14 Proposed model for CSA and HNO <sub>3</sub> doped polyaniline in terms of carrier mobility and the crystallinity	40
4.15 Conductivity vs. PI (%wt) of CSA and HNO <sub>3</sub> doped polyanilines (N <sub>A</sub> /N <sub>EB</sub> = 10, %wt of PI = 1, 5, 10, 20, 30, 50, 70, 75 and 80)	41
4.16 Electrical conductivity response upon exposure to CO at 1000 ppm of CSA doped polyaniline at N <sub>A</sub> /N <sub>EB</sub> = 10	43
4.17 Gas response mechanism of doped polyaniline upon expose to CO	44
4.18 $\Delta\sigma$ vs. [CO] of CSA and HNO <sub>3</sub> doped polyaniline at N <sub>A</sub> /N <sub>EB</sub> = 1	45
4.19 $\Delta\sigma$ vs. [CO] of CSA doped polyaniline at N <sub>A</sub> /N <sub>EB</sub> = 1 and 10	47
4.20 Concentration dependence vs. temperatures of CSA and HNO <sub>3</sub> doped polyaniline at N <sub>A</sub> /N <sub>EB</sub> = 10	50
4.21 $\Delta\sigma$ vs. [CO] of 10-CSA doped polyaniline and 10-CSA doped polyaniline/30 %wt polyimide at 25 °C	53
4.22 $\Delta\sigma$ vs. [CO] of 10-CSA doped polyaniline and 10-CSA doped polyaniline/30 %wt polyimide at 35 °C	53
4.23 $\Delta\sigma$ vs. [CO] of 10-CSA doped polyaniline and 10-CSA doped polyaniline/30 %wt polyimide at 45 °C	54
4.24 $\Delta\sigma$ vs. [CO] of 10-CSA doped polyaniline and 10-CSA doped polyaniline/30 %wt polyimide at 55 °C	54
4.25 $\Delta\sigma$ vs. [CO] of 10-HNO <sub>3</sub> doped polyaniline and 10-HNO <sub>3</sub> doped polyaniline/30 %wt polyimide at 25 °C	55
4.26 $\Delta\sigma$ vs. [CO] of 10-HNO <sub>3</sub> doped polyaniline and 10-HNO <sub>3</sub> doped polyaniline/30 %wt polyimide at 35 °C	55

FIGURE	PAGE
4.27 $\Delta\sigma$ vs. [CO] of 10-HNO <sub>3</sub> doped polyaniline and 10-HNO <sub>3</sub> doped polyaniline/30 %wt polyimide at 45 °C	56
4.28 $\Delta\sigma$ vs. [CO] of 10-HNO <sub>3</sub> doped polyaniline and 10-HNO <sub>3</sub> doped polyaniline/30 %wt polyimide at 55 °C	56
4.29 Proposed model for electron movement of 10-CSA/30% PI and 10-HNO <sub>3</sub> /30% PI at room temperature and at a higher temperature	58
J.1 Ohm's law region of the applied current and the volt drop by using the silicon wafer (Si8-3.5A) as a standard material	92
J.2 Ohm's law regime: the voltage drop and the applied current of the camphorsulfonic acid doped polyaniline (PANI-CSA) and nitric acid doped polyaniline (PANI-HNO <sub>3</sub> ) pellets at doping ratio of $N_A/N_{EB} = 10$	93

**LIST OF SCHEMES**

<b>SCHEME</b>	<b>PAGE</b>
2.1 Polyaniline forms and their interconversions (Stejskal <i>et al.</i> , 1996)	8
3.1 Synthesis path of polyaniline	15
3.2 Synthesis path of polyimide and imidisation process	16
3.3 Conductivity detectors with gas chamber	20
K.1 Linear array four-point probe meter	94